Published in final edited form as:
IEEE Trans Biomed Eng. 2013 August ; 60(8): 2100–2106. doi:10.1109/TBME.2013.2245329.

Evaluation of Optical Coherence Tomography for the Measurement of the Effects of Activators and Anticoagulants on the Blood Coagulation *In Vitro*

Xiangqun Xu,
Department of Chemistry, Zhejiang Sci-Tech University, Hangzhou 310018, China (xuxiangqun@zstu.edu.cn)

Jinhai Geng,
Department of Chemistry, Zhejiang Sci-Tech University, Hangzhou 310018, China (gengjinhai_2007@126.com)

Gangjun Liu, and
Beckman Laser Institute, Department of Biomedical Engineering, University of California, Irvine, CA 92617 USA (gangjunl@uci.edu)

Zhongping Chen
Beckman Laser Institute, Department of Biomedical Engineering, University of California, Irvine, CA 92617 USA (z2chen@uci.edu)

Abstract

Optical properties of human blood during coagulation were studied using optical coherence tomography (OCT) and the parameter of clotting time derived from the 1/*e* light penetration depth ($d_{1/e}$) versus time was developed in our previous work. In this study, in order to know if a new OCT test can characterize the blood-coagulation process under different treatments *in vitro*, the effects of two different activators (calcium ions and thrombin) and anticoagulants, i.e., acetylsalicylic acid (ASA, a well-known drug aspirin) and melagatran (a direct thrombin inhibitor), at various concentrations are evaluated. A swept-source OCT system with a 1300 nm center wavelength is used for detecting the blood-coagulation process *in vitro* under a static condition. A dynamic study of $d_{1/e}$ reveals a typical behavior due to coagulation induced by both calcium ions and thrombin, and the clotting time is concentration-dependent. Dose-dependent ASA and melagatran prolong the clotting times. ASA and melagatran have different effects on blood coagulation. As expected, melagatran is much more effective than ASA in anticoagulation by the OCT measurements. The OCT assay appears to be a simple method for the measurement of blood coagulation to assess the effects of activators and anticoagulants, which can be used for activator and anticoagulant screening.

Index Terms

Anticoagulation; blood coagulation; optical coherence tomography (OCT); 1/*e* light penetration depth

Correspondence to: Xiangqun Xu.

I. Introduction

Coagulation is the process by which blood forms clots. It is an important part of hemostasis, the cessation of blood loss from a damaged vessel, wherein a damaged blood vessel wall is covered by a platelet and fibrin-containing clot to stop bleeding and begin repair of the damaged vessel. Hemostasis of human blood is regulated by the activation of platelets and by a special biochemical blood coagulation system. The inactivated coagulation factors preexist in the blood and are converted into active forms through the influence of activation factors. Disorders of coagulation can lead to an increased risk of bleeding (hemorrhage) or obstructive clotting (thrombosis) [1].

In order to diagnose disorders in these coagulation factors, different biological tests have been developed, such as prothrombin time (PT), partial thromboplastin time (PTT), and activated clotting time (ACT), defined as the necessary time for citrated plasma to clot in the presence of different activators [1]. However, very few of them are performed on blood samples. Existing standard optical tests, used for most of the standard coagulation tests based on the temporal change in optical density, are limited because of blood opacity. The increase in optical density of blood during coagulation is indisputable for plasma samples, as reported in the literature, but is a lot less detectable for blood samples. However, the plasma tests do not precisely reproduce the physiologic event, i.e., the effect of red blood cells (RBCs) in blood as the main component of the blood clot is trapped RBCs by fibrin strands. Many recent studies have also reported the important role of RBCs in the blood-coagulation process [2], [3]. All of these studies have revealed an important need to develop accurate and global standard *in vitro* coagulation tests using blood samples. Therefore, creating methods for blood coagulation monitoring is a matter of great interest.

Optical coherence tomography (OCT) has the major advantage of providing a description of blood properties with high resolution, high sensitivity, and potential application *in vivo*. Blood properties have been widely studied using OCT and Doppler OCT (ODT) due to their high-resolution, real-time, and non-invasive capabilities. OCT relies on short temporal coherence interferometry and measures the optical path and intensity of back-reflected, near-infrared light. Studies of the OCT backscattering signal and ODT variance imaging in characterizing blood optical clearing, hematocrit (HCT), RBCs aggregation, blood photocoagulation, blood oxygen saturation, thrombus volume, and blood fibrinogen level have been reported by us and other groups [4]–[15].

Because the OCT technique measures in-depth intensity distribution with high resolution, changes in the in-depth distribution of the blood-scattering coefficient or refractive index are reflected in changes in the OCT signal [7], [11], [12]. OCT is able to quantify the attenuation coefficient (a result of scattering and absorption). The attenuation property obtained by OCT can be used for the characterization of several different kinds of tissue, and these have been demonstrated by [11] and [16]. Thus, because blood coagulation may introduce local changes in its optical properties (scattering coefficient and local and mean refractive indexes), we recently demonstrated that the $1/e$ light penetration depth ($d_{1/e}$; the point where the signal attenuated to 37% ($1/e$) of the point with the greatest reflectance) is able to differentiate various stages of human blood properties during coagulation induced by 25 mmol/L calcium chloride *in vitro* [17]. In our case, the blood sample is uniform and the $d_{1/e}$ parameter actually represents the attenuation property of the blood sample. In this region, the attenuated power signal within the sample mostly follows the first-order scattering approximation and can be modeled as an exponentially decaying function [18], [19]. The choosing of $d_{1/e}$ parameter ensures that the fitting is accurate. The study provided valuable information regarding the liquid to gel transition of blood during coagulation and also was a means to achieve greater understanding of the specific stages of the process, such

as fibrin formation [17]. The study developed two parameters: 1) clotting time (t_c), defined as the period of time where the 1/*e* light penetration depth curve starts to be stabilized, and 2) rate of fibrin formation (S_r), defined as the slope of $d_{1/e}$ within the period of time where $d_{1/e}$ increases dramatically following the induction of blood coagulation from the variations in $d_{1/e}$ versus time. In order to know if the OCT method can be developed to be a simple, routine, and accurate test for the measurement of blood clot formation that can be used in *in vitro* anticoagulant drug screening and antithrombotic treatment monitoring, this study evaluates the OCT method and parameters to describe changes in the blood-clotting process in different *in vitro* models of coagulation. Dose-dependent effects of two activators of calcium ions and thrombin are studied. Acetylsalicylic acid (ASA), a well-known anticoagulant (aspirin), and melagatran, a direct thrombin inhibitor, are used as model drugs to check the usefulness of the OCT method to characterize the effects of different anticoagulants that have a big difference in effective doses.

Blood coagulation is initiated by Ca^{2+}-dependent binding of the coagulation factor VIIa (FVIIa) to its cofactor, tissue factor (TF). The TF:FVIIa complex activates factors IX and X, ultimately leading to the formation of thrombin and the coagulation of blood. Thrombin, known as factor II in the biochemical pathways of blood coagulation, is generated from prothrombin. Thrombin, in turn, catalyzes the conversion of fibrinogen molecules to fibrin. The polymerization of fibrin in vessels gives rise to thrombus formation. The kinetics of this process depends on thrombin concentration within the plasma. Therefore, calcium ions and thrombin were selected activators to initiate blood coagulation in this study. An initial set of measurements performed in the two models consisting of various concentrations of calcium ions and thrombin in the blood, respectively, was used to establish criteria from the variations in OCT parameters during coagulation. The second set of measurements was performed to identify and quantify variations in OCT parameters related to the two anticoagulants (ASA and melagatran) treatment. Calcium chloride was used to start blood coagulation in these experiments.

II. Materials and Methods

A. Materials

The fresh porcine RBCs and porcine plasma stabilized with sodium citrate were purchased from Animal Technologies, Inc. (Erwin Tyler, TX, USA). The blood samples of HCT in 40% of this study were reconstituted by mixing 0.8 mL RBCs and 1.2 mL plasma or plasma with ASA, and megalatran solution because the anticoagulant drug solution was more easily mixed in plasma rather than in whole blood.

Calcium chloride was dissolved in physiological saline to make a concentration of 0.25 mol/L stock solution. Bovine thrombin (500 IU, T7513, Sigma Chemical, St. Louis, MO, USA) was dissolved in Tris-buffered saline (T5030, Sigma) to a final concentration of 500 IU/mL. Stock solution was stored in small portions (50 μL) for up to one month at −20 °C.

ASA (A3160, Sigma) solution (18.02 mg ASA) was dissolved in 10 mL Tris-buffered saline, giving a concentration of 10 mmol/L. Melagatran (sc-207846, Santa Cruz Biotechnology, Inc., CA, USA) solution (1 mg) was dissolved in 23.3 mL Tris-buffered saline to a concentration of 10 μmol/L.

B. OCT Measurements of the Effects of Activators and Anticoagulants

A swept-source OCT system was used in this study. The system used a compact swept-source laser with a central wavelength of 1310 nm, an A-line rate of 50 kHz, and a total average power of 16 mW (SSOCT-1310, Axsun Technologies, Inc., Billerica, MA, USA).

For the OCT module, a Mach–Zehnder-type interferometer was used, and 90% of the laser light power was sent to the sample arm and 10% of the light to the reference arm. A dual-balanced detection scheme was used to acquire the signal. The system utilized a K-trigger mode so that no linear wavenumber recalibration was needed. In the sample arm, a fiber collimator, a two-axis galvo mirror scanning system and an achromatic doublet with a focal length of 30 mm were used. The system had a beam diameter of 2 mm and a lateral resolution of 14.6 μm. The full-width at half-maximum (FWHM) bandwidth of the laser source was approximately 80 nm, resulting in a depth resolution of 9.3 μm in air [20].

Experiment 1 was performed in the model with calcium chloride as a trigger factor. The reconstituted blood sample described earlier was preincubated at 37 °C. Then, 0.2 mL of calcium chloride solution at the same temperature was added into a 1.8 mL sample of resuspended 0.8 mL RBCs and 1 mL plasma, followed by shaking for 15 s. The influence of three calcium final concentrations (12, 18, and 25 mmol/L) on the reaction process was investigated.

Experiment 2 was performed in the model with thrombin as a trigger factor. The reconstituted blood sample described earlier was preincubated at 37 °C. Then, 20 μL of thrombin was added into a 1.98 mL sample of resuspended 0.8 mL RBCs and 1.16 mL plasma, followed by shaking for 15 s. The influence of four thrombin final concentrations (0.25, 0.5, and 1.0 units/mL) on the reaction process was investigated.

Another two sets of experiments were carried out to determine the effects of ASA (final concentrations of 50, 100, 200, and 300 μmol/L) and melagatran (final concentrations of 0.05, 0.1, 0.2, and 0.4 μmol/L). To obtain a clotting curve, 30 μL ASA or 20 μL melagatran solution was added to 0.47 mL or 0.48 mL plasma (the same plasma was frozen at −20 °C for both ASA and melagatran experiments) and then mixed with 0.4 mL RBCs. The examined sample was preincubated at 37 °C and then 0.1 mL calcium chloride (final concentration, 25 mmol/L) was added to start the process, followed by shaking for 15 s.

Due to these procedures, the start of the OCT measurement was delayed by about 20 s with regard to the onset of the coagulation process. This delay was taken into account by the data evaluation procedure. The control sample, in which calcium chloride, thrombin, ASA, or megalantran solution was replaced with TBS, prepared, and the value acquired immediately after preparation, was used as the value at 0 s for each set experiment.

A rectangular glass cuvette of ∼2 mm height (inner thickness) and 10 mm × 40 mm area was used as a blood sample holder. The sample holder was placed almost perpendicular to the probing beam, but tilted at a small angle of ∼5°, relative to the cell surface to ensure that only light scattered or reflected by blood constituents was detected, and the specular reflection that occurs at the glass-fluid interface was eliminated from the detection system. When the blood sample was added with $CaCl_2$ solution or thrombin as activators, the OCT imaging of the blood sample was acquired immediately. Measuring points were taken every 20 s until 40 min after sampling. A cross-section imaging was obtained by taking 2000 A-scans over 2 mm lateral length. Three experiments for each concentration of all the treatments were carried out.

C. Data Processing

The OCT data were first corrected for system sensitivity roll-off and sample arm optical focusing effect using numerical models described by van Leeuwen *et al*. [21], Faber *et al*. [22], and van Soest *et al*. [23]. The swept-source laser in our system has a coherence length of more than 12 mm and the 3 dB sensitivity roll-off depth is more than 6 mm. In the sample that we have used here, the penetration depth is less than 1 mm and the sensitivity roll-off-

induced intensity change is less than 0.5 dB. The Rayleigh length for the axial point spread function of the current sample arm optics is 0.73 mm. The optical focus is positioned at around 1 mm below the sample surface to enhance the sensitivity in the deeper region. The sensitivity in the shallow region is reduced. This arrangement relaxes the requirement for a high dynamic range of the system, which is a limitation with spectral-domain OCT (SD-OCT) relative to time-domain OCT [24]. The sample surface is placed around the zero-delay position. Quantitative data were then obtained by averaging the signal intensity across the lateral imaging range as a function of depth. Every 500 A-scans were averaged to one depth profile in the OCT imaging. A best-fit exponential curve in depth was applied to the averaged and normalized signal from which the corresponding $1/e$ light penetration depth was derived, as shown in Fig. 1 [25]. A fibrin-time curve was set up by plotting the $d_{1/e}$ values obtained from the entire observation. From the $d_{1/e}$ versus time signals, the clotting time t_c was determined using polynomial fit method and an inflection point was defined as clotting time. The data were the averaged results of triplicates for each sample.

III. Results and Discussion

A. Calcium-Induced Coagulation

Fig. 2 shows the variations in $d_{1/e}$ as a function of time acquired from the blood samples with final concentrations of 0, 12, 18, and 25 mmol/L $CaCl_2$. Two phases could be identified from the three samples with calcium during coagulation, as reported in our previous study [17]. Following the addition of calcium to the blood sample, there was a sharp rise in $d_{1/e}$. The variation in $d_{1/e}$ followed a convex curve to a maximum value. The curves of the variations in the penetration depth can be linked to changes in the state of the medium and coincide with the two stages of a liquid to a solid/gel state. Before $CaCl_2$ solution was added to the blood sample, the medium was in a liquid state. During the first stage (0–t_c), the medium turned into a gel state because of the transformation of fibrinogen into fibrin through a coagulation cascade reaction. In this stage, $d_{1/e}$ increased rapidly. In the second stage (t_c–40 min), variations in $d_{1/e}$ were relatively small, corresponding to the formation of large clot. The results demonstrated that calcium could cause clot formation of blood at the range of 12–25 mmol/L, as investigated in this study. The clotting times (t_c) of 860 ± 30, 720 ± 20, and 620 ± 20 s [as indicated by an arrow in Fig. 2(b)–(d)] were calcium concentration dependent and decreased with the increase in concentration for 12, 18, and 25 mmol/L, respectively. In the plasma test, 12 mmol/L is the concentration used for measuring the recalcification time (RT) that is usually within several minutes. However, the blood sample gave a longer clotting time at the same or even higher concentration of $CaCl_2$. This difference is worthy of being noted for understanding the real physiologic coagulation, i.e., the blood coagulation.

The difference in variations on $d_{1/e}$ between the clotted and nonclotted blood was obvious. For the samples without calcium [see Fig. 2(a)], $d_{1/e}$ increased almost linearly without rising to a plateau within 40 min in agreement with the results of blood during sedimentation [26]. The RBC concentration in the upper layer of the blood sample decreased due to sedimentation, resulting in a decrease in attenuation. In contrast to the nonclotted sample, the fibrin formed from fibrinogen in the blood plasma during blood coagulation may impede the RBC sedimentation.

B. Thrombin-Induced Coagulation

Similar to the results from the samples without calcium, the blood without thrombin showed a continuous increase in $d_{1/e}$ during the 40-min observation caused by RBC sedimentation [see Fig. 3(a)]. The $d_{1/e}$ of the blood with addition of 0.25 IU/mL thrombin also increased with time without reaching saturation but at a lower rising rate than the blood without any

thrombin [see Fig. 3(a)]. This behavior was likely to be an overall result of RBC sedimentation and early coagulation induced by the small amount of thrombin. Two distinct stages of the evolution of $d_{1/e}$ were individualized for the samples activated by thrombin with final concentrations of 0.5 IU/mL [see Fig. 3(b)], 1 IU/mL [see Fig. 3(c)], and 2 IU/mL [see Fig. 3(d)] during blood coagulation on each curve: 1) an increase in $d_{1/e}$, corresponding to the liquid–gel transition of blood, and 2) a plateau with small variations, corresponding to the formation of large clot. The t_c was approximately 1240±20, 1080±20, and 880±20 s for the clotted blood with thrombin of 0.5, 1, and 2 IU/mL, respectively.

It is known that the blood-coagulation process depends on thrombin concentration within the plasma. This study demonstrated that the OCT method was able to detect the clot formation process within the blood rather than in the plasma induced by different doses of thrombin. Furthermore, in the plasma test, a concentration of 0.5 IU/mL thrombin was found to be optimal in clot formation of plasma samples for *in vitro* drug screening [20]. The thrombin concentration (0.5 IU/mL) was considered high enough to directly initiate fibrin formation without exogenous calcium ions added to the sample [27]. Even the lower amounts of 0.125 and 0.25 IU/mL thrombin were sufficient for activation of clot formation in the plasma samples [20]. However, in this study, thrombin at 0.25 IU/mL was not able to induce complete clot formation in the blood samples [see Fig. 3(a)]. Again, it proved that there was an evident difference in coagulation and clot formation between plasma and blood.

During blood coagulation, the fibrinogen is gradually converted to fibrin via a catalytic reaction by the generated throm-bin. Fibrin polymerization finally results in a generation and spatial cross-linking (gel formation) of large fibrin molecules. Depending on shape and size, these molecules give rise to a more or less-intense light scattering, the magnitude of which increases with increasing concentration of these large molecules. Therefore, the optical tests on plasma are performed by recording optical density, light transmission, or light scattering. It is known that upon coagulation, the optical density of the plasma increases, leading to a decrease of the light transmitted through the sample [28]. In contrast to the plasma, light scattering decreased and light penetration in the blood during coagulation increased with an elapse of time (see Figs. 2 and 3). Blood is a scattering system that consists of scattering particles, for example, RBCs and the surrounding media, i.e., plasma. Plasma itself is transparent if coagulation does not occur. Refractive index mismatching between the RBC cytoplasm and plasma is the major source of light scattering in blood [26]. During the blood-coagulation process, the size, dimension, and shape of RBCs do not change. The changes in the scattering resulted from the perturbation in its surrounding environment, i.e., plasma. During coagulation, the fibrinogen in the plasma transformed to coarse fibrin (from 1 nm to 1 μm). The refractive index of the plasma increased with the fibrin formation from 1.34 to 1.40 [17]. The refractive index of the RBCs was measured to be larger than 1.42 [17], [26]. The reduced refractive index mismatching between the RBCs and the plasma led to the decrease in the blood scattering and, thus, to the enhancement of the light penetration depth [7], [10], [26]. Eventually, as most of erythrocytes were trapped in the fibrin meshwork, the clot was formed and the blood tended to be solidified. The transformation led to the corresponding $1/e$ light penetration depth at this moment, i.e., the time point t_c to be stabilized and smaller changes in the $d_{1/e}$. Therefore, although the OCT method for monitoring the blood coagulation induced either indirectly by calcium ions (see Fig. 2) or directly by thrombin (see Fig. 3), as shown in this study, is an optical approach; it actually employs a different principle from that used in the plasma test.

In the second part of this study, experiments with ASA and melagatran were performed to check whether the OCT method for drug screening can be a useful tool to evaluate changes in blood coagulation and clot formation. Calcium chloride at 25 mmol/L was used as an activator.

C. Effect of ASA

Fig. 4 shows the plots of $d_{1/e}$ versus time in the blood samples with ASA at concentrations of 50 μmol/L [see Fig. 4(b)], 100 μmol/L [see Fig. 4(c)], 200 μmol/L [see Fig. 4(d)], and 300 μmol/L [see Fig. 4(e)], including a control sample with no ASA [see Fig. 4(a)]. Similar curves consisting of two phases in the blood with and without ASA during coagulation were obtained. As expected, dose-dependent ASA prolonged t_c [see Fig. 5(a)]. The range of ASA concentrations used in this study was approximate to the maximal plasma concentrations reached after oral administration and to the concentrations (1–1000 μg/mL) used by Buczko *et al*. [29] in *in vitro* experiments.

There are numerous studies substantiating clinical efficacy of ASA as an antithrombotic drug. The primary established effect of ASA on hemostasis is to impair platelet aggregation, thus reducing thrombus formation. A growing body of evidence indicates that ASA may also affect blood coagulation at several levels, thus reducing thrombin generation with the subsequent inhibition of thrombin-mediated coagulant reactions [30]. Although the mechanism of ASA action on plasma coagulation and fibrinolysis factors has not so far been completely elucidated, the simple OCT method presented in this study can be used for measurements of clotting times to assess the effects of anticoagulant ASA on blood.

D. Effect of Melagatran

Levels of $d_{1/e}$ versus time were assayed in the reconstructed blood samples with different amounts of melagatran (0, 0.05, 0.1, 0.2, and 0.4 μmol/L) [see Fig. 6(a)–(e)]. Addition of the direct thrombin inhibitor, i.e., melagatran, to the blood caused a concentration-dependent increase in t_c [see Fig. 5(b)]. When the inhibitor dose was 0.2 μmol/L, which is similar to the peak concentration in plasma following a single oral dose of 24 mg melagatran [31], t_c was approximately prolonged 1.25 times compared to the samples without melagatran. The same effect was caused by ASA at 200 μmol/L [see Fig. 5(a)], which was 1000-fold higher than the dose of melagatran. This observation illustrated that thrombin inhibition induced by melagatran impaired fibrin formation much more effectively than ASA. Hence, we believe that the OCT method is very sensitive in detecting effects of a direct thrombin inhibitor on coagulation. We cannot explain why there was no significant difference in the coagulation effect between 0.05 and 0.1μmol/L. Similar behavior between 0.6 and 0.7 μmol/L in the plasma coagulation was observed in [32]. It should be noted that aspirin is not an obvious choice for a blood sample resuspended of RBCs and plasma with likely low platelet counts. An inhibitor of fibrin polymerization, e.g., pefablock, is more appropriate. In addition, an inhibitor for platelet aggregation, e.g., abciximab, and a naturally occurring peptide in the salivary glands of medicinal leeches, e.g., hiru-dine, were worthy being studied in whole blood. Nevertheless, this study was not aimed to compare different anticoagulants but to evaluate the feasibility of the OCT parameter to differentiate the blood coagulation under different models using activators and anticoagulants.

In this study, the coagulation process in the blood with a physiological HCT of 40% (40–50% in men and 35–45% in women) rather than blood plasma was detected with OCT. Our previous work demonstrated that the coagulation process of blood with HCTs of 35–55% could be characterized by the OCT method. In addition, OCT detection was able to recognize abnormalities in the coagulation rate of the blood with an abnormal low HCT of 25% [17]. Whether the 1/*e* parameter will be transferrable to varying clots because *in vivo* in humans clot composition varies dramatically requires more studies, but an endpoint as 1/*e* parameter is likely to be a simple test for anticoagulant drug screening and antithrombotic treatment monitoring of a patient *in vitro*. For *in vivo* measurements, other parameters such as attenuation coefficient, backscattering coefficient, refractive index, blood flow velocity, and variance of the Doppler frequency spectrum using Doppler OCT [12] may be worthy of

being further studied for better interpretation of clot types. Recently, Faivre *et al*. [33] reported a technique to measure coagulation times relying on the detection of the blood cell immobilization by analysis of the speckle figure resulting from a blood sample. However, the blood was diluted by a coagulation reagent to 1/3 of its original HCT and, thus, did not represent the physiological HCT in the previous study. A light source with 690 nm was not suitable for *in vivo* application either [33].

This study was performed under static conditions. Ongoing studies will show blood coagulation during dynamic conditions monitored by the use of the OCT method because the flow induced shear is a key element of homeostasis, which largely governs the platelet and coagulation activation and, eventually, the formation of a thrombus.

IV. Conclusion

This study demonstrates that the OCT method is a useful and promising tool for the detection of blood-coagulation processes. The blood OCT measurement appears to be superior to the plasma optical density method because it: 1) evaluates coagulation in a physiologic milieu in the presence of RBCs, which are known to modulate blood coagulation; 2) has higher sensitivity; and 3) avoids the extraction of plasma, thus being simpler and faster.

Acknowledgments

This work was supported by in part by the National Natural Science Foundation of China under Grant 81171378; in part by the National Institutes of Health under Grant EB-10090, Grant EY-021519, Grant HL-105215, and Grant EB-015890; in part by the Air Force Office of Scientific Research under Grant FA9550-04-0101; and in part by the Arnold and Mabel Beckman Foundation.

References

1. Lillicrap, D.; Key, N.; Makris, M.; O'Shaughnessy, D. Practical Hemostasis and Thrombosis. Oxford, U.K.: Wiley-Blackwell; 2009.
2. Kaibara M, Iwata H, Ujiie H, Himeno R, Kaibara M. Rheological analyses of coagulation of blood from different individuals with special reference to procoagulant activity of erythrocytes. Blood Coagul. Fibrin. 2005 Jul.vol. 16:355–363.
3. Horne HK, Cullinane AM, Merryman PK, Hoddeson EK. The effect of red blood cells on thrombin generation. Brit. J. Hematol. 2006 May.vol. 133:403–408.
4. Brezinski M, Saunders K, Jesser C, Li X, Fujimoto J. Index matching to improve optical coherence tomography imaging through blood. Circulation. 2001 Aug.vol. 103:1999–2003. [PubMed: 11306530]
5. Blacky JF, Barton JK. Chemical and structural changes in blood undergoing laser photocoagulation. Photochem. Photobiol. 2004 Jul-Aug;vol. 80:89–97.
6. Kirillin MY, Priezzhev AV, Tuchin VV, Wang RK, Myllyl R. Effect of red blood cell aggregation and sedimentation on optical coherence tomography signals from blood samples. J. Phys. D: Appl. Phys. 2005 Aug.vol. 38:2582–2589.
7. Xu X, Wang RK, Elder JB, Tuchin VV. Effect of dextran-induced changes in refractive index and aggregation on optical properties of whole blood. Phys. Med. Biol. 2003 May.vol. 48:1205–1221. [PubMed: 12765332]
8. Iftimia NV, Hammer DX, Bigelow CE, Rosen DI, Ustun T, Ferrante AA, Vu D, Ferguson RD. Toward noninvasive measurement of blood hematocrit using spectral domain low coherence interferometry and retinal tracking. Opt. Exp. 2006 Apr; vol. 14(no. 8):3377–3388.
9. Faber DJ, Mik EG, Aalders MCG, van Leeuwen TG. Toward assessment of blood oxygen saturation by spectroscopic optical coherence tomography. Opt. Lett. 2005 May.vol. 30:1015–1017. [PubMed: 15906988]

10. Xu X, Yu L, Chen Z. Optical clearing of flowing blood using dextrans with spectral domain optical coherence tomography. J. Biomed. Opt. 2008 Feb.vol. 13:021107-1–021107-6. [PubMed: 18465956]
11. Xu X, Yu L, Chen Z. Effect of erythrocyte aggregation on hematocrit measurement using spectral-domain optical coherence tomography. IEEE Trans. Biomed. Eng. 2008 Dec; vol. 55(no. 12): 2753–2758. [PubMed: 19126454]
12. Xu X, Yu L, Chen Z. Velocity variation assessment of red blood cell aggregation with spectral domain Doppler optical coherence tomography. Ann. Biomed. Eng. 2010 Oct.vol. 38:3210–3217. [PubMed: 20473568]
13. Fu F, Xu X, Geng J. Characterization of flowing blood optical property under various fibrinogen levels using optical coherence tomography. IEEE Trans. Biomed. Eng. 2012 Sep; vol. 59(no. 9): 2613–2618. [PubMed: 22801485]
14. Couture L, Richer LP, Cadieux C, Thomson CM, Hossain SM. An optimized method to assess in vivo efficacy of antithrombotic drugs using optical coherence tomography and a modified Doppler flow system. J. Pharmacol. Toxicol. Methods. 2011 Sep.vol. 64:264–268. [PubMed: 21967828]
15. Kuranov RV, Qiu JZ, McElroy AB, Estrada A, Salvaggio A, Kiel J, Dunn AK, Duong TQ, Milner TE. Depth-resolved blood oxygen saturation measurement by dual-wavelength photothermal (DWP) optical coherence tomography. Biomed. Opt. Exp. 2011 Mar.vol. 2:491–504.
16. van der Meer FJ, Faber DJ, Baraznji Sassoon DM, van der Meer FJ, Faber DJ, Baraznji Sassoon DM, Aalders MC, Pasterkamp G, van Leeuwen TG. Localized measurement of optical attenuation coefficients of atherosclerotic plaque constituents by quantitative optical coherence tomography. IEEE Trans. Med. Imaging. 2005 Oct; vol. 24(no. 10):1369–1376. [PubMed: 16229422]
17. Xu X, Lin J, Fu F. Optical coherence tomography to investigate optical properties of blood during coagulation. J. Biomed. Opt. 2011 Sep.vol. 16:096002-1–096002-5. [PubMed: 21950916]
18. Levitz D, Thrane L, Frosz M. Determination of optical scattering properties of highly-scattering media in optical coherence tomography images. Opt. Exp. 2004 Jun.vol. 12:249–259.
19. Xu C, Schmitt JM, Carlier SG, Virmani R. Characterization of atherosclerosis plaques by measuring both backscattering and attenuation coefficients in optical coherence tomography. J. Biomed. Opt. 2008 Mar.vol. 13:034003-1–034003-8. [PubMed: 18601548]
20. Liu G, Jia W, Sun V, Choi B, Chen Z. High-resolution imaging of microvasculature in human skin *in-vivo* with optical coherence tomography. Opt. Exp. 2011 Jul.vol. 26:7694–7705.
21. van Leeuwen TG, Faber DJ, Aalders MC. Measurement of the axial point spread function in scattering media using single-mode fiber-based optical coherence tomography. IEEE J. Sel. Top. Quantum. Electron. 2003 Feb; vol. 9(no. 2):227–233.
22. Faber DJ, van der Meer F, Aalders M, van Leeuwen T. Quantitative measurement of attenuation coefficients of weakly scattering media using optical coherence tomography. Opt. Exp. 2004 Jun.vol. 12:4353–4365.
23. van Soest G, Goderie T, Regar E, Koljenovic´ S, van Leenders GL, Gonzalo N, van Noorden S, Okamura T, Bouma BE, Tearney GJ, Oosterhuis JW, Serruys PW, van der Steen AF. Atherosclerotic tissue characterization in vivo by optical coherence tomography attenuation imaging. J. Biomed. Opt. 2010 Jan.vol. 15:011105-1–011105-5. [PubMed: 20210431]
24. Liu B, Azimi E, Brezinski ME. Improvement in dynamic range limitation of swept source optical coherence tomography by true logarithmic amplification. J. Opt. Soc. Amer. A, Opt. Image Sci. Vis. 2010 Mar.vol. 27:404–414. [PubMed: 20208929]
25. Xu X, Zhu Q. Sonophoretic delivery for contrast and depth improvement in skin optical coherence tomography. IEEE J. Sel. Topics Quantum Electron. 2008 Jan; vol. 14(no. 1):56–61.
26. Tuchin VV, Xu X, Wang RK. Dynamic optical coherence tomography in studies of optical clearing, sedimentation, and aggregation of immersed blood. Appl. Opt. 2002 Jan.vol. 41:258–271. [PubMed: 11900442]
27. Kostka B, Para J, Sikora J. A multiparameter test of clot formation and fibrinolysis for in-vitro drug screening. Blood Coagul. Fibrin. 2007 Oct.vol. 18:611–618.
28. He S, Antovic A, Blomba¨ck M. A simple and rapid laboratory method for determination of haemostasis potential in plasma II. Modifications for use in routine laboratories and research work. Thromb. Res. 2001 Sep.vol. 103:355–361. [PubMed: 11553368]

29. Buczko W, Mogielnicki A, Kramkowski K, Chabielska E. Aspirin and the fibrinolytic response. Thromb. Res. 2003 Jun.vol. 110:331–334. [PubMed: 14592557]

30. Undas A, Brummel-Ziedins KE, Mann KG. Antithrombotic properties of aspirin and resistance to aspirin: beyond strictly antiplatelet actions. Blood. 2007 Dec.vol. 109:2285–2292. [PubMed: 17148593]

31. Ersdal E, Schutzer K, Lonnerstedt C, Ohlsson L, Wall U, Eriksson UG. Plasma concentration of melagatran after ingestion of different doses of the drug. Clin. Drug. Invest. 2005 May.vol. 25:125–133.

32. He S, Zhu K, Mika S, Jenny V, Jan S, Nils E, Margareta B, Hakan W. A global assay of haemostasis which uses recombinant tissue factor and tissue-type plasminogen activator to measure the rate of fibrin formation and fibrin degradation in plasma. Thromb. Haemost. 2007 Oct.vol. 98:871–882. [PubMed: 17938814]

33. Faivre M, Peltie´ P, Planat-Chrétien A, Cosnier M, Cubizolles M, Nougier C, Negrier C, Pouteau P. Coagulation dynamics of a blood sample by multiple scattering analysis. J. Biomed. Opt. 2011 May.vol. 16 057001-1-9.

Biographies

Xiangqun Xu received the B.Sc. degree in biochemistry from Xiamen University, Xiamen, China, in 1985, the M.Sc. degree in biochemistry from Zhejiang Medical University, Hangzhou, China, in 1997, and the Ph.D. degree in biomedical engineering from Keele University, Keele, U.K., in 2003.

She is currently a Professor of Biomedical Engineering at Zhejiang Sci-Tech University, Hangzhou. She received the postdoctoral fellowship in biomedical optics from Cranfield University, Bedford, U.K. Her current research interests include medical imaging, diagnostic spectroscopy, control of optical properties of tissues and blood, and the application of optics in medicine.

Jinhai Geng, photograph and biography not available at the time of publication.

Gangjun Liu, photograph and biography not available at the time of publication.

Zhongping Chen, photograph and biography not available at the time of publication.

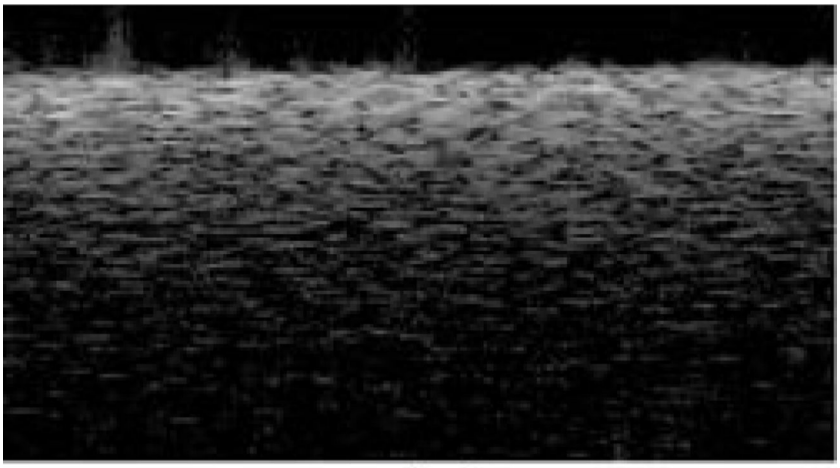

(a)

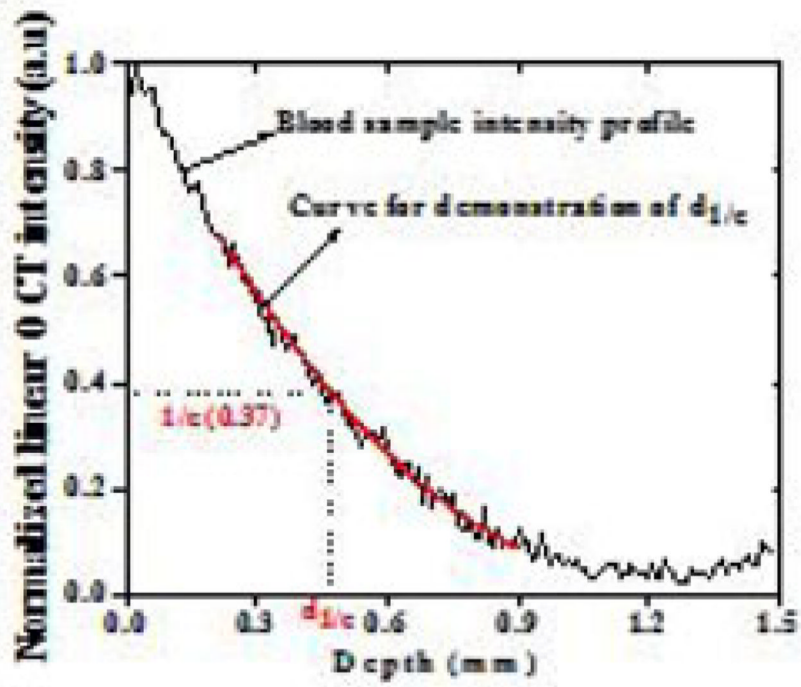

(b)

Fig. 1.

OCT data processing of: (a) OCT image of a blood sample and (b) the curve fit for 1/*e* light penetration depth extraction.

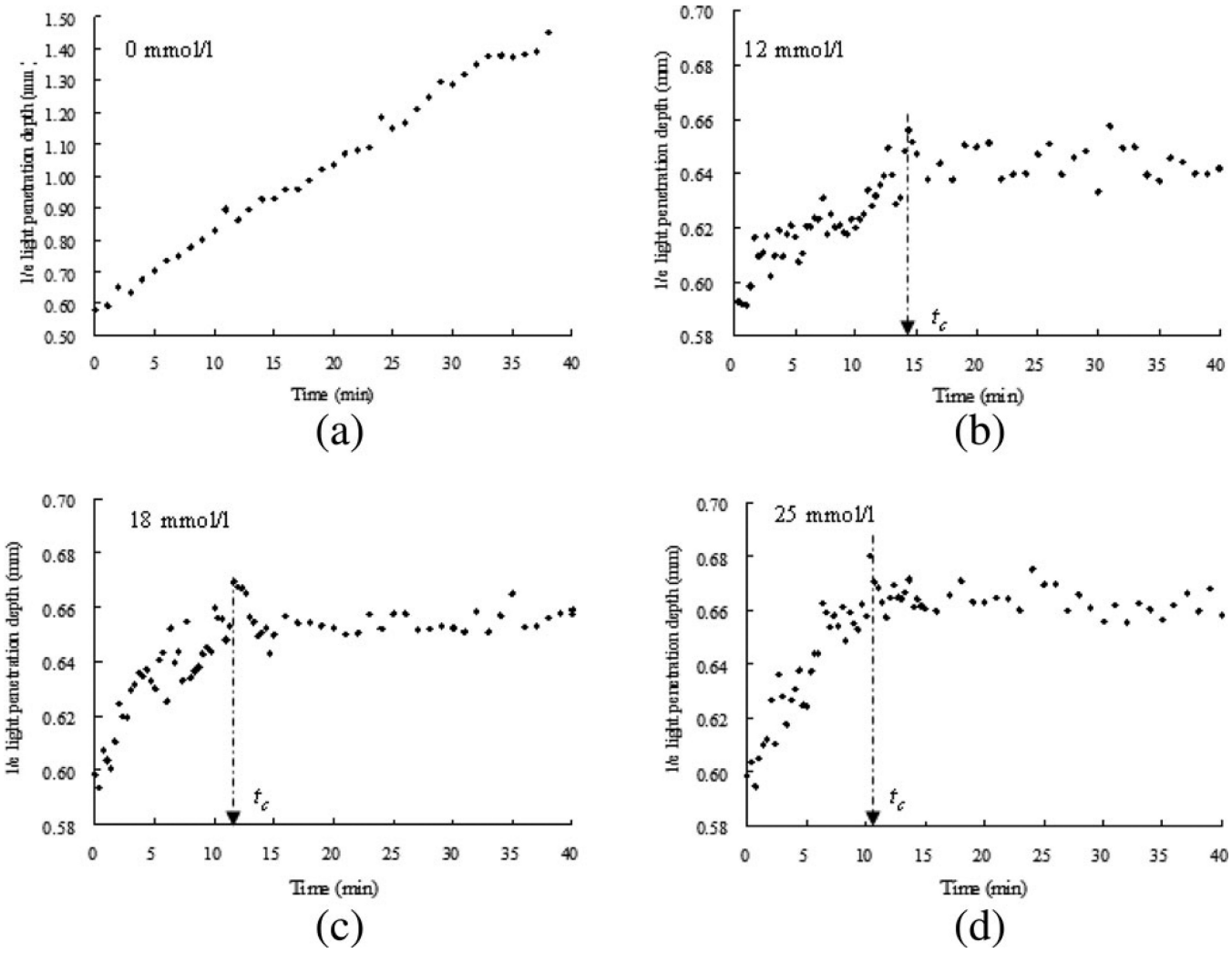

Fig. 2.

$d_{1/e}$ as a function of time obtained from coagulating blood samples induced by 12, 18, and 25 mmol/L calcium chloride, including the samples without calcium ions (n = 3). The clotting time t_c is indicated by an arrow symbol. The clotting time was decreased with the increase of calcium concentration. Measuring points were taken every 20 s up to 15 min and every 1 min from 15 to 40 min.

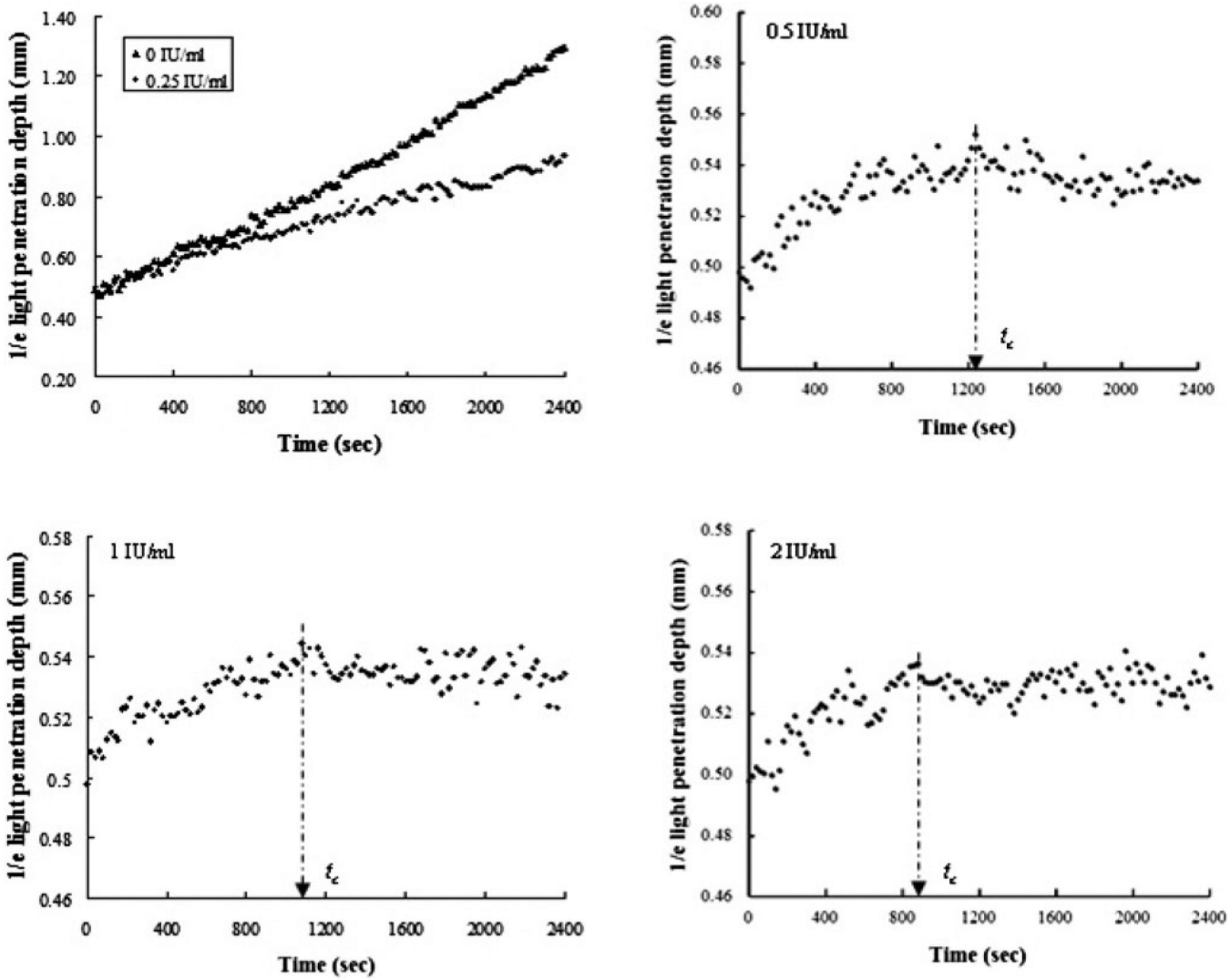

Fig. 3.

Time-course changes in $d_{1/e}$ of the blood samples induced by 0.25, 0.5, 1, and 2 IU/mL thrombin, including the samples without thrombin (n = 3). The clotting time t_c is indicated by an arrow symbol. The clotting time was decreased by the increasing amount of thrombin.

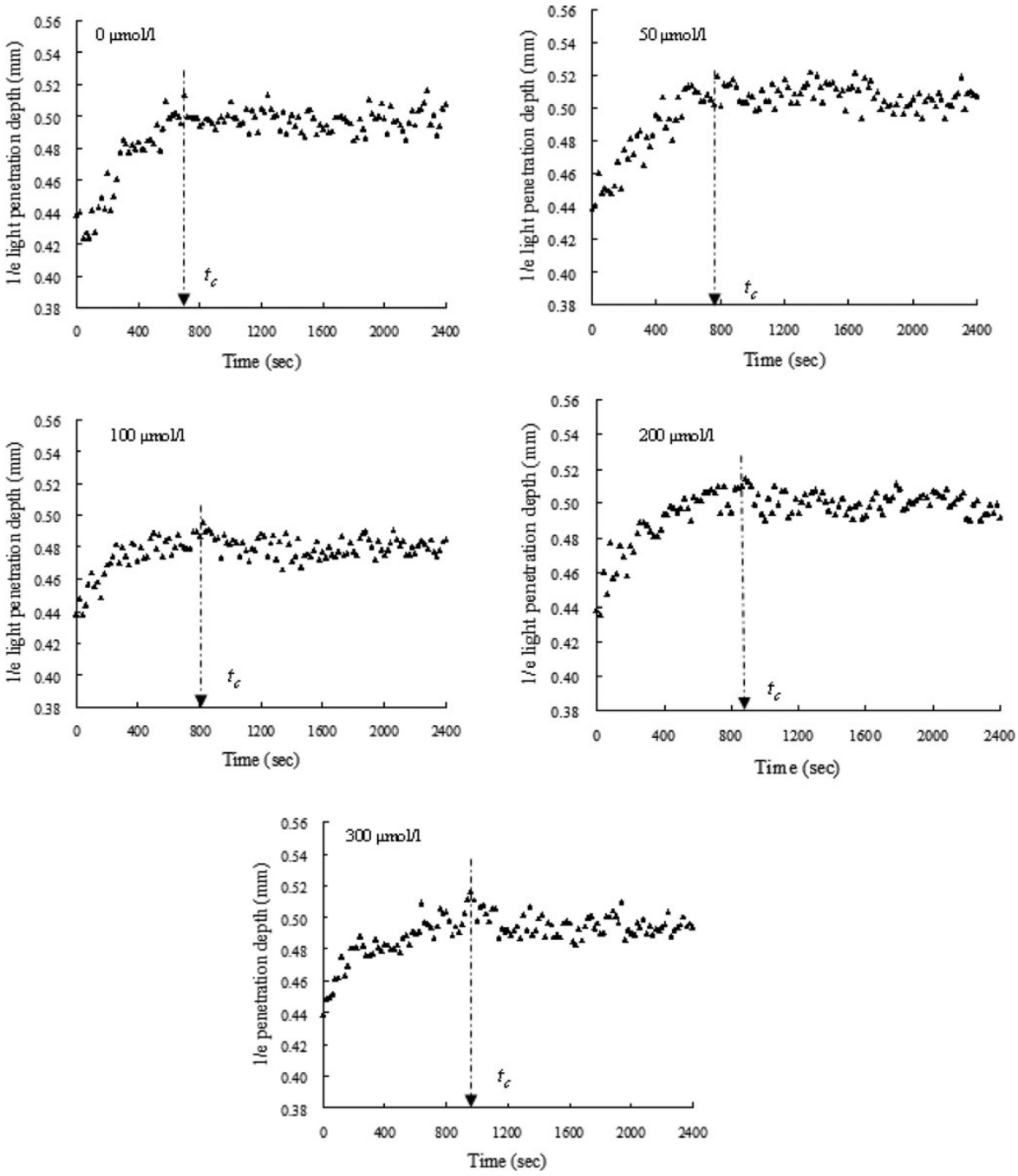

Fig. 4.

Dynamic $d_{1/e}$ of the coagulating blood samples induced by 25 mmol/L calcium chloride with addition of ASA at concentrations of 0, 50, 100, 200, and 300 μmol/L (n = 3). The clotting time was prolonged with the increase of ASA concentration.

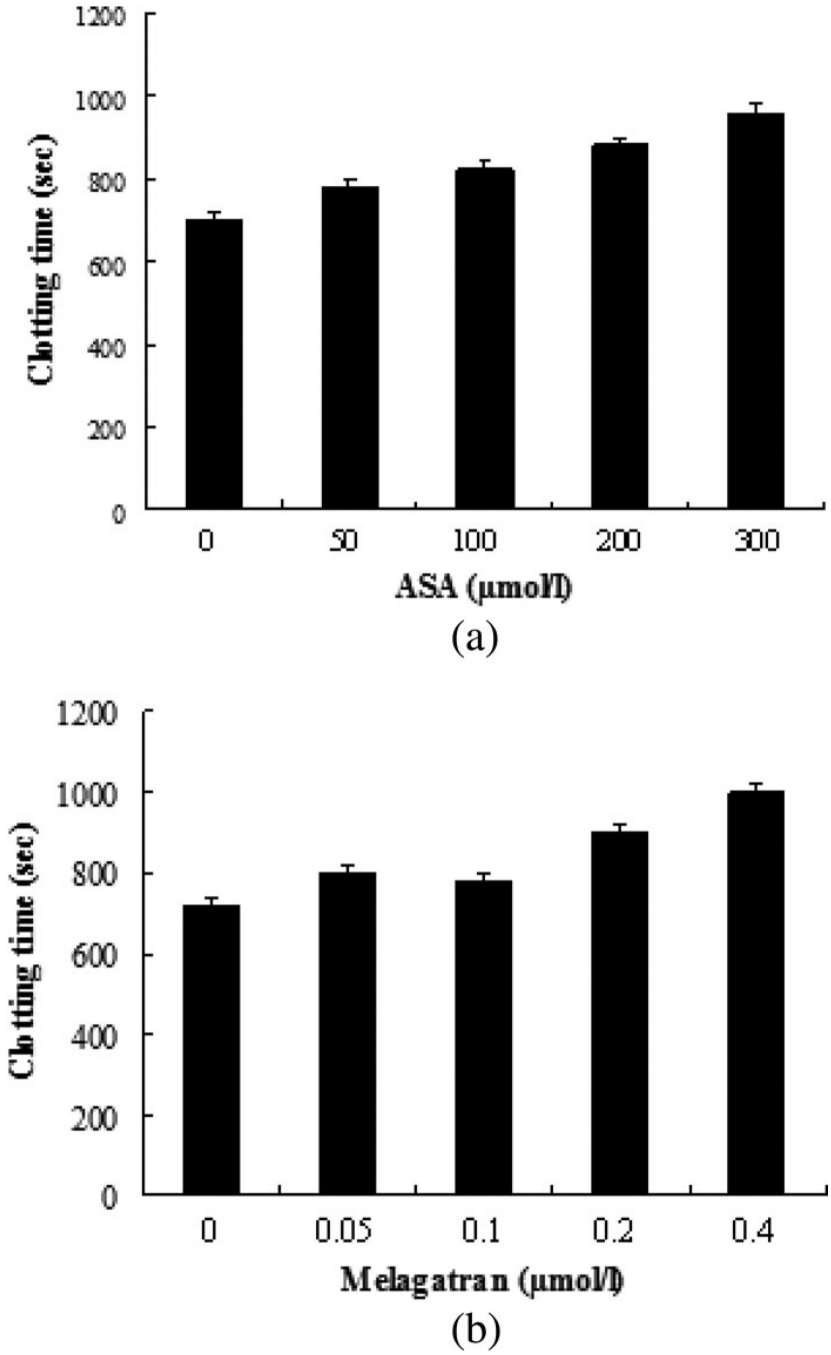

Fig. 5.

Summary of clotting time of the blood samples with different (a) ASA and (b) melagatran (*n* = 3). ASA and melagatran had different effects on blood coagulation.

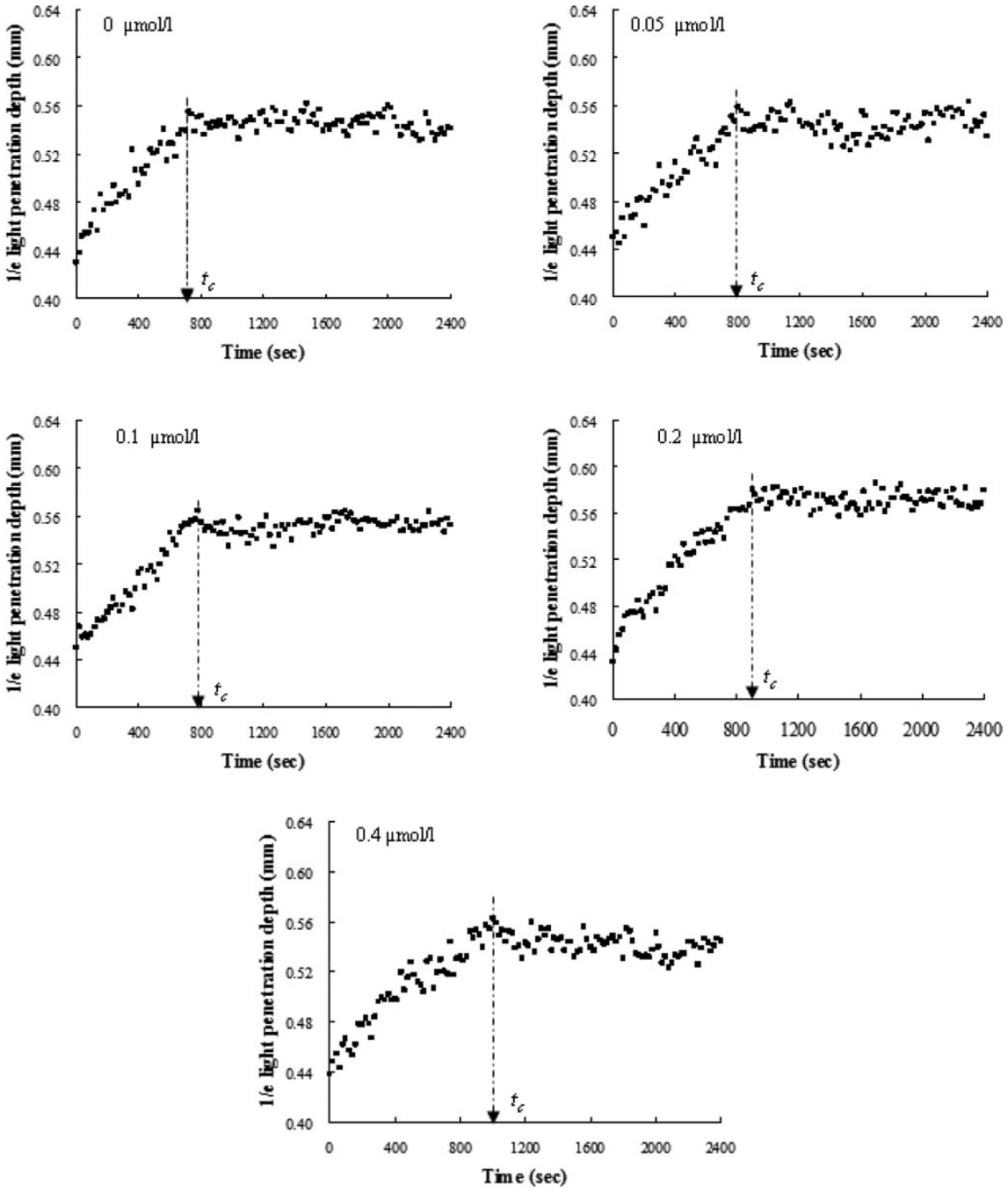

Fig. 6.

Time-course changes in $d_{1/e}$ of the blood samples induced by 25 mmol/L calcium chloride with addition of melagatran at concentrations of 0, 0.05, 0.1, 0.2, and 0.4 μmol/L (n = 3). The clotting time was prolonged with the increasing amount of melagatran.